Journal of Alloys and Compounds 509 (2011) 2203–2215

Contents lists available at ScienceDirect

Journal of Alloys and Compounds

journal homepage: www.elsevier.com/locate/jallcom

Preparation of ZrO_2 and ZrO_2/SiC powders by carbothermal reduction of $ZrSiO_4$

Lj. Kljajević*, B. Matović, A. Radosavljević-Mihajlović, M. Rosić, S. Bosković, A. Devečerski

Materials Science Lab, "Vinča" Institute of Nuclear Sciences, University of Belgrade, P.O. Box 522, 11001, Belgrade, Serbia

ARTICLE INFO

Article history:
Received 21 December 2009
Received in revised form 31 October 2010
Accepted 2 November 2010
Available online 9 November 2010

Keywords:
Ceramics
Gas–solid reactions
Solid state reactions
Microstructure
X-ray diffraction
Scanning electron microscopy

ABSTRACT

This paper is dealing with the synthesis of zirconia/silicon carbide (ZrO_2/SiC) and ZrO_2 powders obtained by carbothermal reduction of natural mineral zircon ($ZrSiO_4$). For the first time, the influence of carbon to $ZrSiO_4$ ratio is thoroughly investigated for a wide range of compositions ($C/ZrSiO_4$ = 1–8) and temperatures (1473–1973 K). The zircon powder was mixed with activated carbon as a reducing agent and heat treated in a controlled flow atmosphere of Ar. Periclase (MgO) was added in order to facilitate the formation of high temperature form of zirconia as well as to examine the possible catalytic effect of MgO on the overall reaction. Phase evaluation and phase content were followed as a function of temperature, $C/ZrSiO_4$ ratio and different quantity of introduced MgO. The obtained powders were characterized by means of ex-situ X-ray diffraction and SEM/EDS investigation. It was found that, depending on $C/ZrSiO_4$ ratio, it is possible to produce either a m-ZrO_2, c-ZrO_2 or ZrO_2/SiC powders by using zircon as precursor.
© 2010 Elsevier B.V. All rights reserved.

1. Introduction

Zirconia and silicon carbide belongs to the group of structural ceramics due to their excellent properties such as high fracture strengths, high temperature resistances, high erosion resistance as well as chemical resistance (1(. However, the commercial application of these ceramics is growing slowly because of the low mechanical reliability of final products. This limitation can be overcome by using biphasic powder mixtures of very hard and very tough compounds such as silicon carbide and zirconia, respectively.

Various routes for preparing engineering ceramics powders have been developed until today. Usually, the best results are obtained by chemical routes, but this method is more costly in terms of industrial manufacturing than conventional milling techniques. Milling is the most common and industrially preferred method of mixing different powders. However, inhomogeneities introduced at this stage remain inside the material and degrade the mechanical properties and reliability of ceramics. It is important to find powders processing routes suitable to produce high homogeneity in powder premixes/mixtures in order to obtain materials with optimal properties.

Carbothermal reduction (CTR) process is promissing candidate for obtaining a great variety of non-oxides products for important technical uses (1(. This method has been used for a long time as a preferred route to process oxidic ores, for the elimination of the silica component in mineral silicates (2–4(. The synthesis of either pure carbide powders or nanocomposite oxide/carbide powders is one of the important factors for obtaining dense non-oxide/oxide technical ceramics. Although the quality and performance are important, the cost of mass production should be the key factor in the commercialization of non-oxide ceramics (5(. The process involves reduction of oxygenated materials, such as silica (SiO_2) by mixing it with a reducing agent (carbon) in excess at the temperatures usually higher than 1873 K, for several hours under an inert atmosphere. Formation of final product is very complex and demands many intermediate stages (6(. This procedure offers the possibility of an economically attractive production route from naturally occurring materials. On the other hand, by using CTR method, obtained powders are usually perfectly homogenized.

Only recently, newly developed/modified methods were used to obtain nanostructural non-oxide powders and composites. Most promising candidates for simple, cost-effective production are: Laser pyrolysis [7]; SHS (self-propagating high-temperature synthesis) [8]; microwave assisted CTR [9]; R.F. induction plasma synthesis [10]; CVI/PIP method (chemical vapor infiltration/polymer infiltration and pyrolysis) [11]; CVC method (chemical vapor condensation) [12,13]; wire explosion method [14].

Considering time/energy consumption, greatest potential lies in SHS method and microwave assisted CTR. Besides, only these two methods are convenient for processing of solid materials such are $ZrSiO_4$ and other naturally occurring minerals. Other methods mentioned above (except wire explosion method, of course), use mainly liquid/gaseous chemicals as a metal precursors.

Despite of relative simplicity and efficiency, the main problem of the SHS method lies in the fact that the final product contains

* Corresponding author. Tel.: +381 11 2439 454; fax: +381 11 2439 454.
E-mail address: ljiljana@vinca.rs (Lj. Kljajević).

0925-8388/$ – see front matter © 2010 Elsevier B.V. All rights reserved.
doi:10.1016/j.jallcom.2010.11.002

impurities originating from the aluminothermic mixture (Al, Mg) needed for self-sustaining SHS reaction.

For microwave assisted CTR the same starting materials are used ($ZrSiO_4$, ZrO_2, SiO_2, carbon) as in "regular" CTR studies (which uses "regular" furnaces to obtain ZrC, SiC, ZrO_2), and the "only" difference being that the samples are heated in a microwave oven. By using the 6:1 carbon/oxide ratio, Das et al. [9] managed to convert $ZrSiO_4$ completely into the ZrC/SiC, within 30 min of irradiation (1673 K).

However, all results and conclusions obtained by "regular" studies (including this one), are/will be applicable for some future SHS and microwave assisted CTR studies (and vice versa), at least when concerning the basic parameters which influence the CTR process of $ZrSiO_4$ and similar solid materials (carbon/oxide ratio, temperature, catalytic effect of additives, etc).

Pure $ZrSiO_4$ decomposes into the ZrO_2 and amorphous SiO_2 at temperatures higher than 1723 K, as it was shown by an extensive *in-situ* study of $ZrSiO_4$ thermal decomposition, performed by Kaiser et al. [15].

$$ZrSiO_4 = ZrO_2 + SiO_2 \quad (1)$$

This study also reveals isostructural transformation of t-$ZrSiO_4$ → t-ZrO_2 in 1723–1973 K temperature region. However, if samples are allowed to cool spontaneously, m-ZrO_2 is obtained. It was also found that the presence of impurities (Al_2O_3, Fe_2O_3, TiO_2, etc) reduces the temperature needed for $ZrSiO_4$ decomposition by formation of low temperature eutectic melts.

It is generally accepted that monoclinic form of ZrO_2 (m-ZrO_2) is stable below 1443 K, tetragonal form (t-ZrO_2) between 1443 K and 2643 K, and cubic form (c-ZrO_2) above 2643 K.

On the other hand, if ZrO_2 is obtained by ZrC oxidation, isostructural transformation c-ZrC → c-ZrO_2 takes place [16]. A considerable amount of carbon was detected in c-ZrO_2 phase, with highest concentration being measured at the ZrC/ZrO_2 interface.

Considering literature data and their own results, Luo et al. [17] also suggests that carbon can help c-ZrO_2 stabilization in two ways: 1 – by surrounding c-ZrO_2 nanoparticles and preventing their aggregation; 2 – by incorporating into the interstitial positions in ZrO_2.

It seems that by preventing the aggregation/growth of ZrO_2 nanoparticles, carbon acts in the way similar to that proposed for Al_2O_3 stabilized ZrO_2 [18,19]. By coating the ZrO_2 nanoparticles with Al_2O_3 layer, their growth is suppressed and due to the high surface tension in ZrO_2 nanoparticles [17,20,21], t(c)-ZrO_2 structure is retained at low temperatures.

High surface tension is also responsible for appearance of tetragonal phase at room temperature in undoped zirconia nanoparticles [7,22].

Reaction of carbothermal reduction of zircon is strongly dependent on the amount of added carbon [2,7,23–27], i.e. by varying the C/$ZrSiO_4$ ratio, it is possible to obtain ZrO_2, ZrO_2/SiC or ZrC/SiC as reaction products:

$$ZrSiO_4 + C = ZrO_2 + SiO_{(g)} + CO_{(g)} \quad (2)$$

$$ZrSiO_4 + 3C = ZrO_2 + SiC + 2CO_{(g)} \quad (3)$$

$$ZrSiO_4 + 6C = ZrC + SiC + 4CO_{(g)} \quad (4)$$

Other experimental parameters like heating/cooling rate, static/dynamic atmosphere, presence of impurities, could also affect the reaction. For example, form of obtained ZrO_2 (monoclinic, tetragonal, cubic) seems to be dependent on the cooling rate, presence of excess carbon, presence of additives and/or impurities, etc. However, different experimental conditions used in different studies make comparison of available data rather difficult, because of very limited range of C/$ZrSiO_4$ compositions investigated in published studies.

Formation of SiC from silica is usually represented by following general reaction:

$$SiO_{2(s)} + 3C_{(s)} = SiC_{(s)} + 2CO_{(g)} \quad (5)$$

Formation of final product is far more complex than the above equation shows, since (depending on experimental conditions) the process of SiC formation may consist of a series of solid–solid, solid–gas and gas–gas reactions, (3,6,28,29(:

$$SiO_{2(s)} + C_{(s)} = SiO_{(g)} + CO_{(g)} \quad (6)$$

$$C_{(s)} + SiO_{(g)} = Si_{(s,l)} + CO_{(g)} \quad (7)$$

$$Si_{(s,l)} + C = SiC + CO_{(g)} \quad (8)$$

$$SiO_{2(s)} + CO_{(g)} = SiO_{(g)} + CO_{2(g)} \quad (9)$$

$$C_{(s)} + CO_{2(g)} = 2CO_{(g)} \quad (10)$$

$$SiO_{(g)} + 3CO_{(g)} = SiC + 2CO_{2(g)} \quad (11)$$

$$3SiO_{(g)} + CO_{(g)} = SiC + 2SiO_2 \quad (12)$$

Formation of ZrC from zirconia is usually represented by following general reaction:

$$ZrO_2 + 3C = ZrC + 2CO_{(g)} \quad (13)$$

Eq. (13) is also an oversimplified view for the far more complex mechanism of ZrO_2 carbothermal reduction [2,24,27,30], which comprise steps similar to those presented for SiC (Eqs. (6)–(12)).

Reaction for the complete carbothermal reduction of zircon (4) thus represents the sum of reactions (5) and (13).

It is also found that the rate of SiO_2 carbothermal reduction reaction increase with increasing the carbon content [23]. In addition, an excess of carbon is preferred in order to suppress the loss of material by undesired reactions like the one presented by Eq. (14):

$$SiC + SiO_2 = 3SiO_{(g)} + CO_{(g)} \quad (14)$$

Excess of carbon should also prevent occurrence of undesired reactions like that presented by reaction (15), which can also lead to the loss of material during the CTR reaction of $ZrSiO_4$:

$$3SiC + 2ZrO_2 = 2ZrC + 3SiO_{(g)} + CO_{(g)} \quad (15)$$

Reaction (15) is possible because formation of SiC precedes ZrC formation. According to experimental observations and thermodynamical predictions based on free-energy calculations [2,24,27,30], formation of SiC is favored at lower temperatures than formation of ZrC, thus making SiC an effective reducing agent for ZrO_2 CTR reaction.

De Souza and Terry [2], observed that addition of MgO, CaO, Y_2O_3 facilitated formation of t-ZrO_2, but also that catalytic effect of these additives on the carbothermal reduction of $ZrSiO_4$ (isothermal conditions), decreased in order: MgO > Y_2O_3 > CaO > no additive.

It is important to underline that most of the reactions proposed in the literature, considering CTR processes of different materials, are *descriptive* in nature. This means that their existence is *assumed* on the basis of changes observed (usually by XRD) in system. So, they *should not* be treated like exact (absolutely precise) equations, especially when considering that their occurrence is usually without thermodynamic support, which also indicates that the *true* mechanisms are *much more complex.* In other words, by using wrong (imprecise, erroneous) chemical equations, the wrong thermodynamic data will be obtained. Besides that, thermodynamic calculations do not include kinetic factors like catalytic influence of liquid phase on the material transport etc. As a result, not even TMD calculations are guarantee that some reaction will or will not occur. Reactions like ((3)–(5) and (13)) can be, and they are used in practice in a stoichiometric manner, i.e. by mixing 1 mol of SiO_2 with 3 mol of C you should convert all SiO_2 into the SiC. But these

reactions are *summary reactions* of very complex many-step mechanisms, and they *only describe starting* and *final* stage of the process, *saying nothing* about what happens during the course of the reaction. Therefore, all reactions presented in further text should be taken primarily as descriptive, and to some extent, stoichiometric.

As previously mentioned, although significant number of studies concerning $ZrSiO_4$ CTR process exists, there is still a need for one consistent and detailed study, in order to completely resolve influence of $C/ZrSiO_4$ ratio on the reaction products, and that was the primary goal of this work. Secondary goal was to prove that it is beneficial to use an excess of carbon, not only to prevent the undesired loss of material (Eqs. (14)–(15)), but first of all, to convert all ZrO_2 into the ZrC which then can be easily converted into the c-ZrO_2 by simple oxidation of ZrC. Tertiary goal was to examine the possible influence of MgO addition on the $ZrSiO_4$ decomposition, course of CTR process (non-isothermal conditions) and stabilization of high temperature forms of ZrO_2.

2. Experimental

Commercially available zircon powder ($ZrSiO_4$, "Trebol", USA, ~40 μm) was used as the starting material. Chemical analysis of the powder, given by the manufacturer, is as follows: ZrO_2 – 65%, SiO_2 – 33%, Al_2O_3 – 2%, TiO_2 – 0.35%, Fe_2O_3 – 0.05%. Periclase powder (MgO, "Zorka", Serbia) was first calcined at 1173 K in order to remove any moisture and surface carbonates, and than mixed with $ZrSiO_4$ powder (5, 10 and 30 wt.% respectively to zircon powder). Activated carbon dried at 383 K (2 h) was used as a reducing agent ("Trayal", Serbia, ~10 μm, ashes ≤1%, specific surface area BET ~1000 $m^2\,g^{-1}$, AC in further text).

The $C/ZrSiO_4$ mixtures were prepared by mixing $ZrSiO_4$ with appropriate amounts of AC in order to obtain samples with various molar ratios ($C/ZrSiO_4$ = 1–8).

Previously prepared $ZrSiO_4$/MgO powder mixtures were also mixed with appropriate quantities of activated carbon in order to obtain the ratio of 7 mol of carbon per 1 mol of the zircon, i.e. the presence of excess carbon when considering reaction (4).

Carbothermal reduction of samples is performed in the 1473–1973 K temperature range (graphite crucibles, heating rate = 40 K/min, Ar flow atmosphere, 1 h soaking time, bed thickness ≈1 cm) in a water-cooled vertical graphite furnace ("ASTRO", Santa Barbara, USA). Samples were furnace cooled to the room temperature under the Ar flow (typically 2–3 h, depending on soaking temperature), removed from the furnace and decarburized at 873 K (2 h) in air, in order to obtain ZrO_2 from ZrC and also to remove any unreacted carbon.

Structural analysis (XRD) was carried out by a Siemens D-500 XRD powder diffractometer with CuK_α radiation (in conjunction with CuK_β nickel filter) on the products before and after decarburization process. The average crystallite size, was calculated from Scherrer's formula [31]:

$$\%\langle D\rangle = \frac{0.9\lambda}{(\beta\cos\theta)} \tag{16}$$

where $\langle D\rangle$ is the average crystallite size, λ is the wavelength of the X-rays, θ is the diffraction angle, $\beta = (\beta_m^2 - \beta_s^2)$, β is corrected half width, β_m observed half width and β_s is half-width of the standard Si sample (provided by Siemens).

Phase composition of samples is represented in a fairly standard semi-quantitative way, by comparing intensities of the main (strongest) reflection for each phase. For example: $ZrSiO_4$ (1 0 0) – means that main $ZrSiO_4$ reflection is the strongest reflection in whole XRD spectrum; m-ZrO_2 (25) – means that the intensity of the main m-ZrO_2 reflection is 25% of the intensity of the strongest reflection in spectrum ($I_{m-ZrO_2}/I_{ZrSiO_4} = 0.25$); SiC (t) – means that the main reflection of SiC phase is observable, but to weak to be accurately measured (t = traces). SiC (u) – means that SiC phase is present, but it cannot be accurately measured due to the overlapping with reflections of some other phase (u = undetermined).

The microstructural study and energy dispersive analysis of X-rays (EDS) were performed by JEOL 6300F scanning electron microscope (SEM) on samples with Au coating.

3. Results and discussion

Due to the mentioned complex nature of the $ZrSiO_4$ CTR reaction and strong dependence on the experimental conditions used, we first evaluate the behaviour of starting $ZrSiO_4$ powder and $ZrSiO_4$/MgO mixtures (without carbon addition) in graphite crucibles at elevated temperatures.

The XRD patterns of samples are presented in Fig. 1. XRD pattern of $ZrSiO_4$ heat treated in graphite crucible at 1673 K (Fig. 1b) shows no difference when comparing with pattern of starting $ZrSiO_4$ powder (Fig. 1a). However, by raising the temperature to 1773 K (Fig. 1f), $ZrSiO_4$ starts to decompose into the monoclinic m-ZrO_2 (JCPDS No. 36-0420) and SiO_2 (Eq. (1)). Because no reflections of SiO_2 are observed, it can be assumed that SiO_2 phase is amorphous similar to what was observed by Kaiser et al. [15] and Das et al. [9]. The SiO_4-tetrahedra in $ZrSiO_4$ are structurally disconnected and obtained SiO_2 is therefore amorphous. This clearly shows catalytic influence of carbon (i.e. graphite crucible) on the $ZrSiO_4$ thermal decomposition, which should normally occur at ≈1950 K. This claim is further supported by XRD pattern of $ZrSiO_4$ heat-treated in an Al_2O_3 crucible at 1773 K (Fig. 1g), which shows only $ZrSiO_4$ reflections, and no trace of ZrO_2 phase i.e. no sign of $ZrSiO_4$ decomposition.

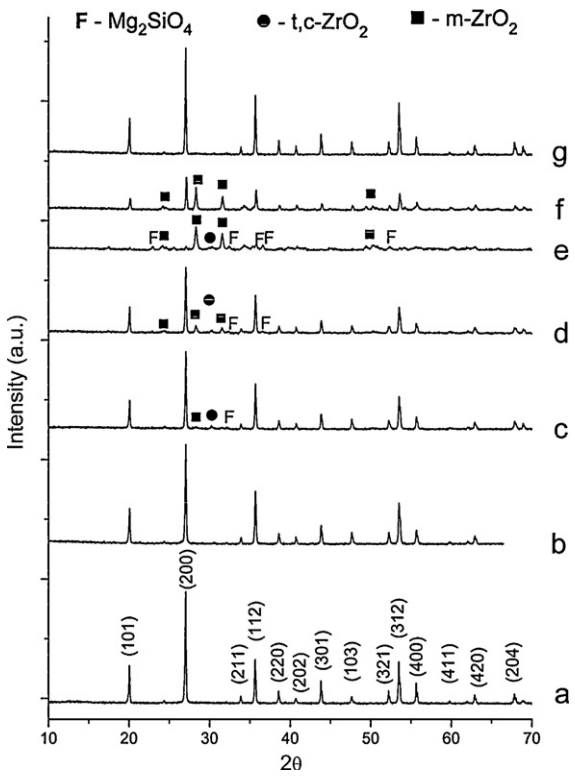

Fig. 1. The XRD patterns of samples without carbon addition: a – $ZrSiO_4$, b – $ZrSiO_4$ (1673 K), c – $ZrSiO_4$/5% MgO (1673 K), d – $ZrSiO_4$/10% MgO (1673 K), e – $ZrSiO_4$/30% MgO (1673 K), f – $ZrSiO_4$ (1773 K), g – $ZrSiO_4$ (1773 K, Al_2O_3 crucible).

XRD patterns of samples containing 5%, 10% and 30% of MgO (Fig. 1c–e, respectively) heat treated in graphite crucibles at 1673 K, show catalytic influence of MgO on $ZrSiO_4$ decomposition. MgO reacts with $ZrSiO_4$ and produces forsterite (Mg_2SiO_4, JCPDS No. 34-0189) and ZrO_2. Sample with 30% of MgO shows almost no presence of $ZrSiO_4$, because 30 wt.% of MgO correspond to ≈2 mol of MgO:

$$ZrSiO_4 + 2MgO \rightarrow Mg_2SiO_4 + ZrO_2 \tag{17}$$

i.e., by chemical reaction with 2MgO, $ZrSiO_4$ is converted into the Mg_2SiO_4 and m-ZrO_2.

It can also be seen that small amounts of tetragonal t-ZrO_2 (JCPDS No. 17-0923) and/or cubic c-ZrO_2 (JCPDS No. 27-0997) are formed in these samples, probably because some Mg-ions entered the ZrO_2 lattice and thus stabilized the high temperature ZrO_2 phase. Due to the weak intensities of reflections, it is impossible to determine which high-temperature form of ZrO_2 is present. Higher MgO content → higher m-ZrO_2 and Mg_2SiO_4 contents (Fig. 1c–e).

In addition, it should be noted that all samples heat-treated in graphite crucibles are light-grey in color, in contrast to cream-white color of starting $ZrSiO_4$ powder and cream color of $ZrSiO_4$ heated at 1773 K in Al_2O_3 crucible. Grey color did not disappear even after exposing the samples to air at 873 K. Since we know

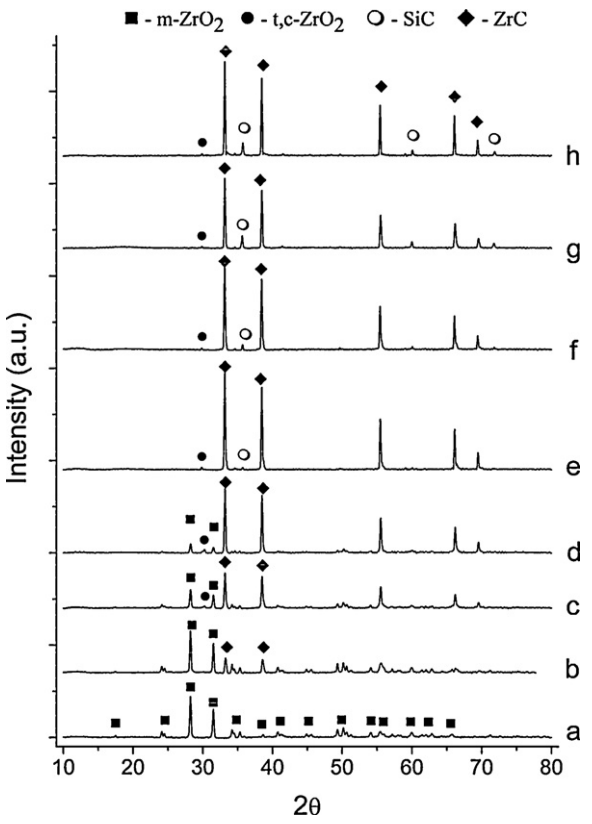

Fig. 2. XRD patterns of samples with different $C/ZrSiO_4$ molar ratios heat treated at 1873 K: (a) 1:1; (b) 2:1; (c) 3:1; (d) 4:1; (e) 5:1; (f) 6:1; (g) 7:1; (h) 8:1.

that SiC is already forming at these temperatures, it is grey in color and stable in air at 873 K, we can conclude that light-grey color of samples may originate from SiC formed on the surface of $ZrSiO_4$ particles, due to the reaction of the $ZrSiO_4$ powder with graphite crucible. SiC reflections are not observed presumably due to: (a) the overlapping with reflections of a dominant crystalline $ZrSiO_4$ phase; (b) small amount of SiC formed. Experimentally observed weight loss (4.6 wt.%) for $ZrSiO_4$ sample heat treated at 1773 K in graphite crucible, confirms the existence of $ZrSiO_4$/graphite reaction. On the other hand, samples that are heat-treated at 1673 K in graphite crucibles, together with sample heat treated in Al_2O_3 crucible at 1773 K, show no observable weight loss. This clearly indicates how important materials (crucibles) used are, i.e. their influence on the $ZrSiO_4$ decomposition temperature, and it is a good example that every detail must be taken into account, when discussing and making conclusions on CTR reactions of $ZrSiO_4$. This finding was important to note, because in literature we observe that graphite and ceramic crucibles are equally often used in investigations of decomposition process/CTR reaction of $ZrSiO_4$ and similar materials.

Next step was to evaluate the influence of carbon content on $ZrSiO_4$ CTR reaction. Influence of $C/ZrSiO_4$ ratio on phase content of $ZrSiO_4$ CTR reaction products can be clearly seen from XRD patterns of samples heat treated at 1873 K (Fig. 2):

Fig. 2a – $C/ZrSiO_4$ = 1:1; only m-ZrO_2 phase is present.
Fig. 2b – $C/ZrSiO_4$ = 2:1; m-ZrO_2 phase dominant, ZrC formed.
Fig. 2c – $C/ZrSiO_4$ = 3:1; ZrC phase dominant, m-ZrO_2, traces of t,c-ZrO_2 phase.
Fig. 2d – $C/ZrSiO_4$ = 4:1; ZrC phase dominant, m-ZrO_2 phase still present, traces of t,c-ZrO_2 phase.
Fig. 2e – $C/ZrSiO_4$ = 5:1; ZrC phase dominant, traces of t,c-ZrO_2 and SiC phase, no trace. of m-ZrO_2 phase

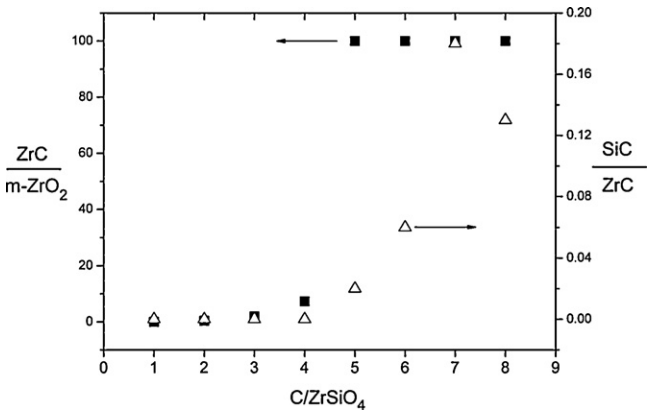

Fig. 3. Change in phase content for samples presented in Fig. 2.

Fig. 2f–h – $C/ZrSiO_4$ = 6:1, 7:1, 8:1; ZrC phase dominant, traces of t,c-ZrO_2 phase, SiC phase clearly present

The change in phase content is more conveniently presented in Fig. 3, using comparison of the intensity ratios of strongest reflections for existing phases (for example: $I_{ZrC}/I_{m\text{-}ZrO_2} = x$; where $x = 0$ means that ZrC phase is absent, and $x = 100$ means that m-ZrO_2 phase is absent).

As one can see from Figs. 2 and 3, amount of ZrC formed increases with increasing amount of carbon added, reaching its maximum in sample with $C/ZrSiO_4$ = 5:1, i.e. in this sample the whole amount of m-ZrO_2 is consumed and transformed into the ZrC. It is also important to note that in this sample SiC appears for the first time. The absence of the SiC reflections in samples with $C/ZrSiO_4 < 5:1$, means that total amount of SiC formed is used as reducing agent in ZrC synthesis, as represented by reaction (15). After the whole amount of m-ZrO_2 is transformed into the ZrC, remaining SiC phase appears in XRD spectrum. Further support is given by the fact that from this point forward, SiC content increases with increasing carbon content, and reaches its maximum in sample with 7:1 molar ratio.

These observations are important because it is now absolutely clear that in sample with $C/ZrSiO_4$ = 3:1, CTR reaction of $ZrSiO_4$ does not proceed as proposed by reaction (3). In samples with $C/ZrSiO_4$ = 2:1–5:1, formation of SiC, represented by reaction (3) i.e. reaction (5), is only the first step of the reaction, followed immediately by reaction (15).

From the observed increase in SiC content in samples with $C/ZrSiO_4 \geq 5:1$, following important conclusions arise:

- at 5:1 ratio almost pure ZrC is obtained with only traces of SiC, which implies that pure ZrC can be obtained by varying carbon content around this point.
- at 1873 K, reactions (13) and (15) are obviously competitive in nature (equally favorable by thermodynamic/kinetic conditions in our system), and that's why SiC content is higher in samples with 6:1, 7:1 and 8:1 ratio, than in sample with 5:1 ratio. If it would not be so, the SiC content would be the same as in sample with 5:1 ratio. In another words, if more carbon is present – more SiC will "survive", because ZrO_2 will consume carbon that surrounds it, instead of SiC.

XRD patterns of samples heat treated at 1873 K and then decarburized in air (873 K, 2 h) are presented in Fig. 4.

Phase composition of decarburized samples as observed from their XRD patterns:

Fig. 4a – $C/ZrSiO_4$ = 1:1; only m-ZrO_2 phase is present.
Fig. 4b – $C/ZrSiO_4$ = 2:1; m-ZrO_2 phase dominant, c-ZrO_2 formed.

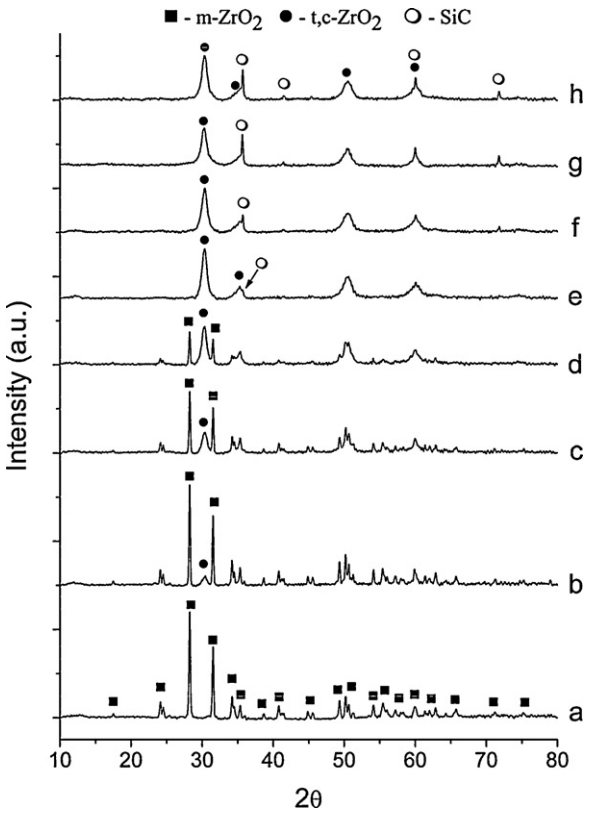

Fig. 4. XRD patterns of samples heat treated at 1873 K after decarburization process: (a) 1:1; (b) 2:1; (c) 3:1; (d) 4:1; (e) 5:1; (f) 6:1; (g) 7:1; (h) 8:1 C/$ZrSiO_4$ ratio.

Fig. 4c – C/$ZrSiO_4$ = 3:1; m-ZrO_2 phase dominant, c-ZrO_2.
Fig. 4d – C/$ZrSiO_4$ = 4:1; c-ZrO_2 and m-ZrO_2 phase.
Fig. 4e – C/$ZrSiO_4$ = 5:1; c-ZrO_2 phase dominant, trace of SiC phase, no trace of m-ZrO_2 phase.
Fig. 4f–h – C/$ZrSiO_4$ = 6:1, 7:1, 8:1; c-ZrO_2 phase dominant, SiC phase clearly present.

Obviously, oxidation at 873 K transforms ZrC into the c-ZrO_2 in all samples. The m-ZrO_2 phase is present only in samples where m-ZrO_2 was present before decarburization process. It can also be seen that reflections of c-ZrO_2 are much wider than those of preceding ZrC (≈0.2° for ZrC and ≈0.9° for c-ZrO_2) indicating that crystallites in c-ZrO_2 are much smaller than those in ZrC ($\langle D\rangle \approx 10$ nm for c-ZrO_2, and $\langle D\rangle \approx 40$ nm for ZrC). Moreover, the calculated average crystallite sizes for c-ZrO_2 phase in our samples, are in very good agreement with those observed by Shimada (2–10 nm) using HRTEM [16], for c-ZrO_2 samples obtained also by ZrC oxidation.

The change in phase content is more conveniently presented in Fig. 5, using intensity ratios of strongest reflections for phases compared.

The change in phase composition of samples after oxidation in air, presented in Fig. 5, is similar to that of samples before oxidation (Fig. 3), simply because they are closely related with their predecessors: the only change is that now complete amount of ZrC is converted into the c-ZrO_2 [16], while other phases are unaltered by oxidation process. For example, in sample with 5:1 ratio, m-ZrO_2 completely disappeared and first sign of SiC formation is observed, similarly to observations made for the 5:1 sample before oxidation.

More details about $ZrSiO_4$ CTR reaction can be found by closer examination of XRD patterns for samples with 4:1 and 5:1 ratio, in temperature range 1673–1973 K, before (Figs. 6 and 7) and after (Figs. 8 and 9) decarburization process.

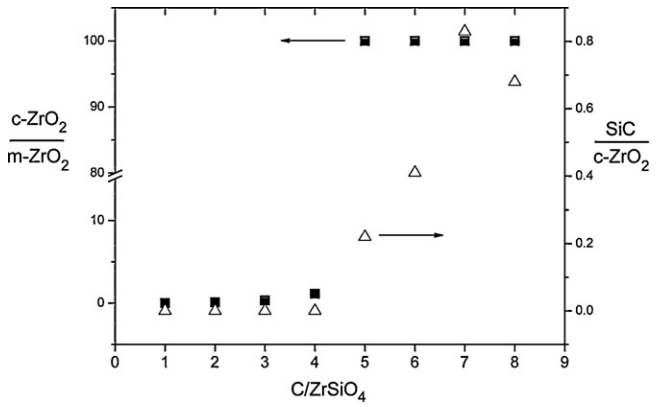

Fig. 5. Change in phase content for samples presented in Fig. 4.

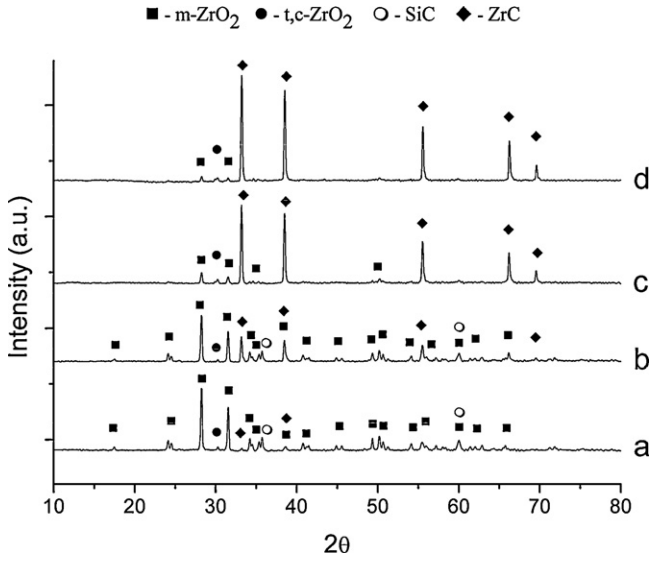

Fig. 6. XRD patterns of sample with 4:1 C/$ZrSiO_4$ ratio heat treated at: (a) 1673 K; (b) 1773 K; (c) 1873 K; (d) 1973 K.

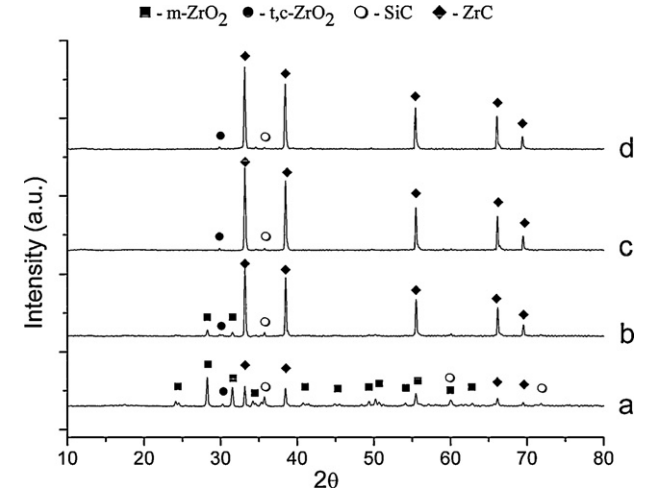

Fig. 7. XRD patterns of sample with 5:1 C/$ZrSiO_4$ ratio heat treated at: (a) 1673 K; (b) 1773 K; (c) 1873 K; (d) 1973 K.

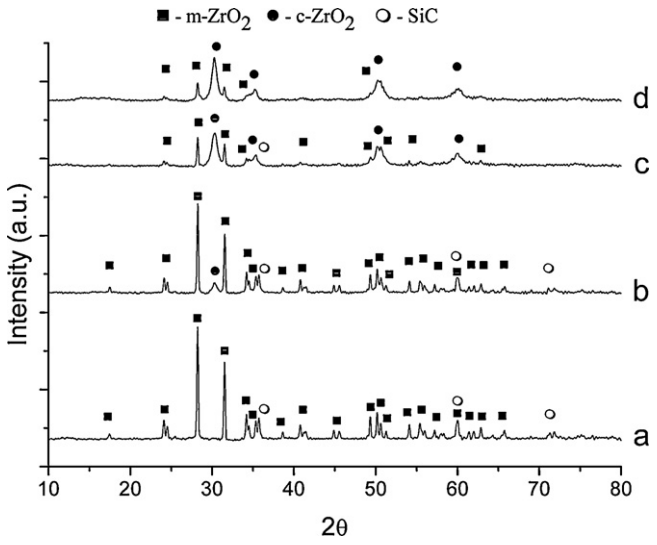

Fig. 8. XRD patterns for samples with 4:1 C/$ZrSiO_4$ ratio, heat treated at different temperatures and then submitted to decarburization process (873 K, air): (a) 1673 K; (b) 1773 K; (c) 1873 K; (d) 1973 K.

From XRD patterns presented in Figs. 6 and 7, several very important observations can be made:

- ZrC phase appears at 1673 K. There are only traces of ZrC in sample with 4:1 ratio, but it is definitely present in sample with 5:1 C/$ZrSiO_4$ ratio. Obviously, at this temperature, there are favorable conditions for development of carbothermal reduction of m-ZrO_2. No trace of $ZrSiO_4$ phase were observed.
- m-ZrO_2 phase content in sample with 4:1 ratio decreases with increasing temperature but it is present at all temperatures. Presence of m-ZrO_2 at 1973 K indicates that all carbon and SiC are consumed during the process. The intensity of SiC reflections also decreases with increasing temperature. The absence of SiC phase in patterns at 1873 and 1973 K confirms that SiC is consumed in during the process of m-ZrO_2 carbothermal reduction (Eq. (15)).
- SiC phase content in sample with 5:1 ratio also decreases with increasing temperature. However, SiC traces can be observed at 1873 and 1973 K. The presence of SiC in this sample at 1873 and 1973 K confirms our assumption that reactions (13) and (15) are competitive, i.e. sufficient amount of carbon in this sample makes "survival" of SiC phase possible. Another evidence for this assumption can be seen when comparing m-ZrO_2 phase content in patterns for 4:1 and 5:1 samples: at all temperatures, m-ZrO_2 phase content is much lower in samples with 5:1 ratio, and finally, at 1873 K m-ZrO_2 phase completely disappeared, i.e. m-ZrO_2 is completely transformed into the ZrC due to sufficient amount of carbon in this sample.
- Small amount (traces) of t,c-ZrO_2 can be observed in both samples at all temperatures. Formation of small amount of stabilized t,c-ZrO_2 can be explained by the presence of the impurities (for example, 2 wt.% of Al_2O_3 in starting $ZrSiO_4$ powder). It is also obvious that the t,c-ZrO_2 phase is more resistant to carbothermal reduction than m-ZrO_2. Due to the weak intensities of reflections, it is impossible to distinguish which high-temperature form of ZrO_2 is present (tetragonal or cubic).

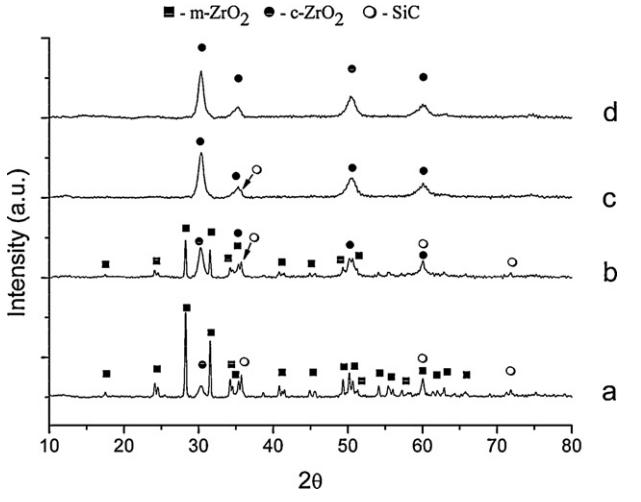

Fig. 9. XRD patterns for samples with 5:1 C/$ZrSiO_4$ ratio, heat treated at different temperatures and then submitted to decarburization process (873 K, air): (a) 1673 K; (b) 1773 K; (c) 1873 K; (d) 1973 K.

From XRD patterns of samples after the decarburization process (Figs. 8 and 9), following observations can be made:

- ZrC phase is completely converted into the c-ZrO_2. No traces of unreacted ZrC were observed.
- m-ZrO_2 phase content in sample with 4:1 ratio decreases with increasing temperature but it is present at all temperatures. The c-ZrO_2 phase appears at 1773 K, at the same temperature at which ZrC appeared in significant amounts. At 1673 K the c-ZrO_2 could not be observed due to the small amount of ZrC formed in sample before decarburization.
- m-ZrO_2 phase in sample with 5:1 ratio disappears at 1873 K, as already observed for the same sample before decarburization. The c-ZrO_2 phase appears at 1673 K, i.e. at the same temperature at which ZrC appeared in sample before decarburization.

It is now easier to observe the presence of SiC phase which is clearly present in both samples at 1873 K and lower temperatures, while its presence is hard to observe in samples at 1973 K due to overlapping its reflection with c-ZrO_2 broad reflection. However, the presence of SiC phase can be deduced by the change in color. All samples are light-grey in color except the sample with 4:1 ratio heat treated at 1973 K, which is creamy in color. The creamy color indicates that there is no SiC phase in 4:1 sample, because the color of pure SiC (90–99.8% purity) can vary from dark-grey to light-grey or green. Contrary to that, grey color of 5:1 sample indicates that SiC phase is still present in this sample, i.e. this sample is not really pure c-ZrO_2 phase as it seems by observations made solely on the basis of the XRD pattern.

Actually, the color of the samples is quite indicative when concerning phase composition of samples i.e. the progress of CTR reaction, as it can be observed from Table 1, in which the phase composition and the color of samples are presented as a function of temperature and C/$ZrSiO_4$ ratio. The phase composition is represented by intensity of strongest reflection of each phase in XRD pattern, as explained before.

SiC phase is hard to observe in XRD patterns of samples with lower carbon content at $T \leq 1673$ K, where SiC and $ZrSiO_4$ phase coexist together, because the main reflection of SiC overlapped with strong reflection of $ZrSiO_4$ phase. However, light-grey color of samples after decarburization process suggests that SiC phase is present in these samples. Formation of SiC at this temperature is observed in numerous studies considering the CTR process of SiO_2 and Mg-silicates [3,6,28,29,32–34]. At higher temperatures, main SiC reflection is usually quite distinguishable from weaker nearby reflections of m-ZrO_2 and c-ZrO_2. In samples with higher SiC content, the presence of reflection at $2\theta \approx 72^\circ$ is also used as an evidence for undoubted presence of SiC. However, coexistence of SiC and $ZrSiO_4$ phases makes determination of SiC content impossible.

Table 1
Phase composition and color of the samples.

	1673 K	Decarb.	1773 K	Decarb.	1873 K	Decarb.	1973 K	Decarb.
1:1	$ZrSiO_4$ (100) m-ZrO_2 (29) Dark-grey	$ZrSiO_4$ (100) m-ZrO_2 (24) Light-grey	$ZrSiO_4$ (100) m-ZrO_2 (44) Dark-grey	$ZrSiO_4$ (100) m-ZrO_2 (45) Light-grey	m-ZrO_2 (100) Dark-grey	m-ZrO_2 (100) Light-grey	m-ZrO_2 (100) Dark-grey	m-ZrO_2 (100) Cream
2:1	m-ZrO_2 (100) $ZrSiO_4$ (85) Dark-grey	$ZrSiO_4$ (100) m-ZrO_2 (83) Light-grey	m-ZrO_2 (100) $ZrSiO_4$ (14) Dark-grey	m-ZrO_2 (100) $ZrSiO_4$ (17) Light-grey	m-ZrO_2 (100) ZrC (36) Black	m-ZrO_2 (100) c-ZrO_2 (9) Light-grey	m-ZrO_2 (100) ZrC (54) Black	m-ZrO_2 (100) c-ZrO_2 (11) Cream
3:1	m-ZrO_2 (100) $ZrSiO_4$ (35) SiC (u) Dark-grey	$ZrSiO_4$ (100) m-ZrO_2 (18) SiC (u) Light-grey	m-ZrO_2 (100) ZrC (12) SiC (12) c-ZrO_2 (t) Dark-grey	m-ZrO_2 (100) SiC (12) c-ZrO_2 (4) Light-grey	ZrC (100) m-ZrO_2 (51) c-ZrO_2 (7) Black	m-ZrO_2 (100) c-ZrO_2 (31) Light-grey	ZrC (100) m-ZrO_2 (18) c-ZrO_2 (t) Black	m-ZrO_2 (100) c-ZrO_2 (56) Cream
4:1	m-ZrO_2 (100) SiC (21) c-ZrO_2 (5) ZrC (4) Dark-grey	m-ZrO_2 (100) SiC (20) Light-grey	m-ZrO_2 (100) ZrC (54) SiC (23) c-ZrO_2 (4) Dark-grey	m-ZrO_2 (100) SiC (20) c-ZrO_2 (10) Light-grey	ZrC (100) m-ZrO_2 (14) c-ZrO_2 (5) Black	c-ZrO_2 (100) m-ZrO_2 (87) Light-grey	ZrC (100) m-ZrO_2 (4) c-ZrO_2 (t) Black	c-ZrO_2 (100) m-ZrO_2 (43) Cream
5:1	m-ZrO_2 (100) ZrC (71) SiC (32) c-ZrO_2 (7) Black	m-ZrO_2 (100) SiC (26) c-ZrO_2 (14) Light-grey	ZrC (100) m-ZrO_2 (9) SiC (6) c-ZrO_2 (t) Black	m-ZrO_2 (100) c-ZrO_2 (80) SiC (43) Light-grey	ZrC (100) SiC (t) c-ZrO_2 (t) Black	c-ZrO_2 (100) SiC (18) Light-grey	ZrC (100) SiC (t) c-ZrO_2 (t) Black	c-ZrO_2 (100) SiC (u) Light-grey
6:1	ZrC (100) m-ZrO_2 (53) SiC (29) c-ZrO_2 (12) Black	m-ZrO_2 (100) SiC (38) c-ZrO_2 (33) Light-grey	ZrC (100) SiC (9) c-ZrO_2 (t) Black	c-ZrO_2 (100) SiC (56) m-ZrO_2 (32) Light-grey	ZrC (100) SiC (6) c-ZrO_2 (t) Black	c-ZrO_2 (100) SiC (41) Light-grey	ZrC (100) SiC (8) c-ZrO_2 (t) Black	c-ZrO_2 (100) SiC (43) Light-grey
7:1	ZrC (100) m-ZrO_2 (21) SiC (29) c-ZrO_2 (5) Black	m-ZrO_2 (100) SiC (96) c-ZrO_2 (90) Light-grey	ZrC (100) SiC (15) c-ZrO_2 (6) Black	SiC (100) c-ZrO_2 (81) Light-grey	ZrC (100) SiC (18) c-ZrO_2 (t) Black	c-ZrO_2 (100) SiC (84) Light-grey	ZrC (100) SiC (22) c-ZrO_2 (t) Black	c-ZrO_2 (100) SiC (87) Light-grey
8:1	ZrC (100) m-ZrO_2 (44) SiC (27) c-ZrO_2 (9) Black	m-ZrO_2 (100) SiC (46) c-ZrO_2 (41) Light-grey	ZrC (100) SiC (13) c-ZrO_2 (t) Black	c-ZrO_2 (100) SiC (69) Light-grey	ZrC (100) SiC (13) c-ZrO_2 (t) Black	c-ZrO_2 (100) SiC (68) Light-grey	ZrC (100) SiC (8) c-ZrO_2 (t) Black	c-ZrO_2 (100) SiC (38) Light-grey

Decarb. – after decarburization process (873 K, 2 h, air); t – traces; u – impossible to determine due to the overlapping;

The initial color of all as-prepared C/$ZrSiO_4$ powder mixtures was black. As one can see, general rule is that decarburized samples are lighter in color than their predecessors. Color of samples before decarburization is black or dark-grey. Color of decarburized samples is light-grey or creamy.

Samples with 5:1, 6:1, 7:1 and 8:1 C/$ZrSiO_4$ ratios remains black after CTR reaction at 1673–1973 K. This indicates the presence of free (excess) carbon in all of these samples.

Contrary to that, dark-grey color of samples with 1:1, 2:1, 3:1 and 4:1 ratios at 1673 and 1773 K, indicates that the part of the carbon is consumed in CTR process at these temperatures, because color is changed from starting black into the dark-grey. However, most interesting observation is that at 1873 and 1973 K, the color of these samples turns black again. This can be explained by increased content of ZrC in these samples at 1873 and 1973 K, because it is known that fine ZrC powders are black in color. As we already said, average crystallite size for ZrC in our samples is $\langle D \rangle \approx 40$ nm, which indicates possible existence of very fine ZrC particles.

On the other hand, majority of the decarburized samples is light-grey in color, with exception of samples heat treated at 1973 K with 1:1, 2:1, 3:1 and 4:1 ratios (creamy color).

The creamy color of samples is as we already explained, indication that SiC phase is absent i.e. consumed by CTR reaction (Eq. (15)). It is also important to notify again that the pure $ZrSiO_4$ sample heat treated at 1773 K in Al_2O_3 crucible (Fig. 1g) is creamy in color.

Regarding phase content of samples, presented in Table 1, it is noticeable that higher carbon content in samples have beneficial effect on the CTR reaction, as already seen from Figs. 3 and 5. The ZrC (c-ZrO_2) content increases with increasing carbon content and temperature. The SiC content seems to have maximum for 7:1 C/$ZrSiO_4$ ratio. The carbon content higher than 7:1 and temperatures higher than 1873 K, seems to have no significant effect on both ZrC and SiC phase contents.

For samples with lower carbon content, decarburization process gives either pure m-ZrO_2 (sample with 1:1 ratio, 1973 K) or mixture of m-ZrO_2/c-ZrO_2 (samples with 2:1, 3:1 and 4:1 ratio, 1973 K). In samples with higher carbon content ($\geq$5:1; 1873–1973 K), resulting products are mixture of c-ZrO_2 and SiC.

Also, low SiC content in sample with 5:1 ratio indicates that it should be possible to obtain pure c-ZrO_2 by slightly varying the carbon content and time/temperature of heat treatment. This may also lead to pure ZrC powders (with no free carbon in it), or at least to ZrC powders with minimal free carbon presence. By varying the same parameters in samples with higher C/$ZrSiO_4$ ratios, it may be also possible to obtain ZrC/SiC powders with the presence of the minimum free carbon. Both ZrC/SiC and c-ZrO_2/SiC powders are interesting because they offer the possibility to be used latter for synthesis of ZrC/SiC and c-ZrO_2/SiC composite ceramics. However, the extent of investigations needed in order to obtain precise answers to these questions, largely surpasses the frame (goals) of the present study, and will be the scope of our future studies.

The only thing that seems to lack the proper explanation is the change in m-ZrO_2/$ZrSiO_4$ ratio after the decarburization of samples with 2:1 and 3:1 ratios heat treated at 1673 K. As one can see from Table 1, after oxidation in air, $ZrSiO_4$ phase became dominant over m-ZrO_2 phase. This is fully expressed in sample with 3:1 ratio i.e. in sample with higher carbon content. Since there is no change

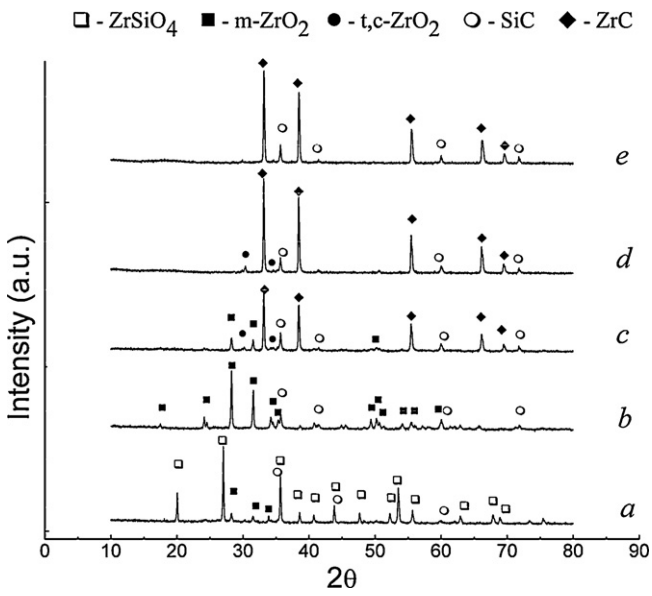

Fig. 10. The XRD patterns of samples with C/$ZrSiO_4$ ratio = 7:1, after been subjected to carbothermal reduction at: (a) 1473 K, (b) 1573 K, (c) 1673 K, (d) 1773 K, (e) 1873 K.

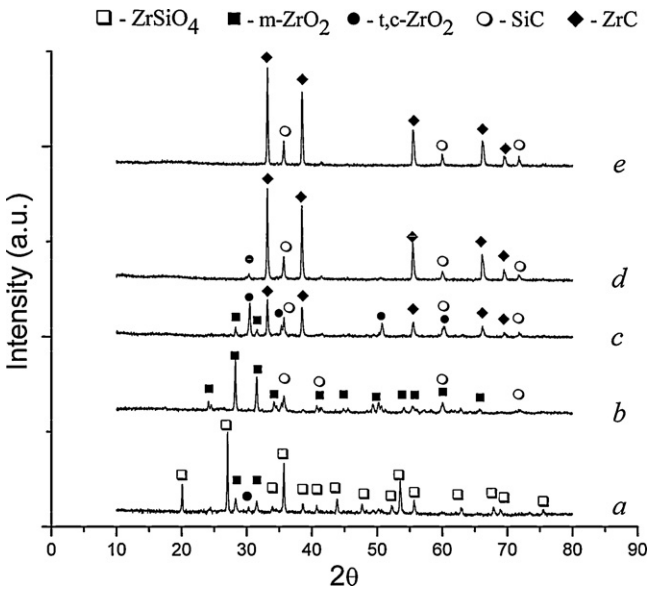

Fig. 11. The XRD patterns of samples with 5% MgO addition, after been subjected to carbothermal reduction at: (a) 1473 K, (b) 1573 K, (c) 1673 K, (d) 1773 K, (e) 1873 K.

in width of the m-ZrO_2 and $ZrSiO_4$ reflections (i.e. in crystallinity of samples) before/after oxidation, while the increased intensities of $ZrSiO_4$ reflections are obvious, it suggests that $ZrSiO_4$ content is increased indeed in samples after oxidation i.e. after reaction with oxygen. Decarburization temperature (873 K) is obviously too low for recombination of decomposition products (m-ZrO_2 and SiO_2, Eq. (1)) into the $ZrSiO_4$, since temperature needed for $ZrSiO_4$ formation is at least 1673 K [15]. It seems that observed phenomenon can be logically explained only by assuming that some kind of oxycarbide ($ZrSiO_xC_y$) intermediary phase exists after CTR reaction at 1673 K, which is then transformed back into the $ZrSiO_4$ due to the reaction with oxygen at 873 K. This can also explain why the change in m-ZrO_2/$ZrSiO_4$ content ratio is stronger in 3:1 than in 2:1 sample: higher carbon content = more oxycarbide formed. Further support for this assumption is found in the fact that formation of similar intermediate oxycarbide phase (ZrO_xC_y) is observed for CTR reaction of ZrO_2 (C/$ZrSiO_4$ ratio = 3:1) at 1623–1823 K [30]. Similarly to our case, if this oxycarbide phase is further reacted with carbon, it turns into the ZrC, but if exposed to oxygen at $T \geq 573$ K, it turns back into the ZrO_2.

Influence of MgO on $ZrSiO_4$ CTR reaction was evaluated with samples obtained by mixing the $ZrSiO_4$/MgO powders with appropriate amounts of carbon in order to obtain the samples with C/$ZrSiO_4$ ratio = 7:1. We decided to use this ratio on the basis of results presented in Table 1. The reason seems to be the content of SiC which is maximum in samples with the mentioned ratio.

First, we are going to closer examine the XRD patterns of sample with 7:1 ratio without MgO addition. Fig. 10 shows the XRD patterns of samples with C/$ZrSiO_4$ = 7:1 after the carbothermal reduction at different temperatures. XRD pattern of sample heated at 1473 K (Fig. 10a) shows the presence of $ZrSiO_4$ and m-ZrO_2. The presence of SiC reflections cannot be reliably proved due to their overlapping with reflections of a dominant crystalline $ZrSiO_4$ phase. The intensity of m-ZrO_2 reflections increases when increasing heating temperature to 1573 K (Fig. 10b). The $ZrSiO_4$ reflections disappeared, and reflections of β-SiC (JCPDS No. 29-1129) are now clearly visible. Comparing with the data presented in Fig. 1b–f, it is obvious that high carbon content leads to further decrease in $ZrSiO_4$ decomposition temperature (Fig. 10b – complete decomposition achieved at 1573 K; Fig. 1f – incomplete decomposition at 1773 K). Because only SiC and m-ZrO_2 phase are detected at 1573 K, it is obvious that decomposition of $ZrSiO_4$ is caused by reaction with carbon (Eqs. (2)–(3)).

Taking into account the 7:1 molar ratio, decomposition of $ZrSiO_4$ at 1573 K in the presence of carbon, as observed from XRD patterns, can be approximately represented by following equation:

$$ZrSiO_{4(s)} + 7C_{(s)} = ZrO_{2(s)} + SiC_{(s)} + 2CO_{(g)} + 4C_{(s)} \quad (18)$$

The weight loss for the reaction (18) is expected to be 21 wt.% and experimentally observed weight loss at 1573 K is 27.3%. Before comparing these values, we must take into account the following facts: (a) the overall process is far more complex (Eqs. (6)–(12), for example); (b) some $SiO_{(g)}$ can be lost from system due to working conditions (Ar flow atmosphere); (c) activated carbon itself loses weight during the thermal treatment, due to the decomposition of active surface groups and evolution of the gaseous products (CO; CO_2; OH; etc).

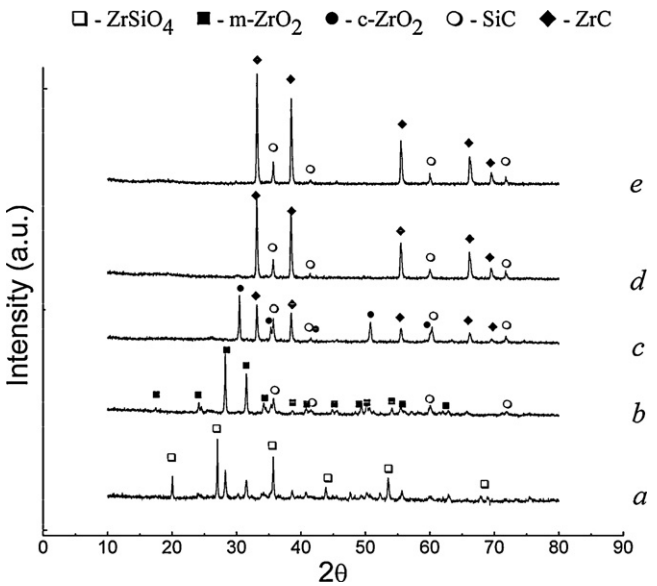

Fig. 12. The XRD patterns of samples with 10% MgO addition, after been subjected to carbothermal reduction at: (a) 1473 K, (b) 1573 K, (c) 1673 K, (d) 1773 K, (e) 1873 K.

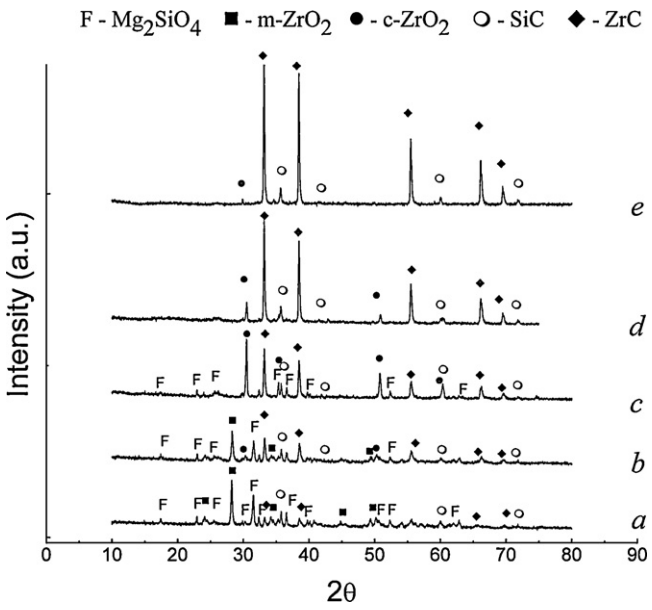

Fig. 13. The XRD patterns of samples with 30% MgO addition, after been subjected to carbothermal reduction at: (a) 1473 K, (b) 1573 K, (c) 1673 K, (d) 1773 K, (e) 1873 K.

Although we cannot influence the first two factors, we can measure the weight loss of our activated carbon. Weight loss of dried activated carbon after heat treatment at 1473 K (Ar, 1 h) is 16 wt.%, and further increase in temperature seems to have no significant effect on the weight loss. After including activated carbon weight loss in our calculations, the obtained value for expected weight loss will be 26 wt.%, which is in very good agreement with experimentally observed weight loss (27.3 wt.%). This indicates that although CTR reactions are very complex, some stoichiometric predictions could be made, if all known (measurable) parameters are included.

We need to emphasize this finding, because the weight loss is often used in the literature as a criterion for the validity of assumed chemical equations. Since majority of studies that we found in the literature, seem to neglect the weight loss of carbon materials themselves, we must underline the fact that the *real* carbon materials possess carbon atoms with unsaturated bonds, which are usually saturated by oxygen, thus producing surface groups. The only exceptions are fullerenes and nanotubes, which are close-caged structures with no unsaturated bonds. If carbon material possess large amount of surface groups (like activated carbon and similar materials with high specific surface and/or chemically activated surface), and especially in samples with high carbon content, weight loss due to the thermal decomposition of these surface groups must be taken into account. The same rule applied for all substances that lose from their own weight during the heat treatment.

At 1673 K (Fig. 10c), dominant phase is ZrC (JCPDS No. 35-0784). Weak reflections of SiC and m-ZrO_2 are also present, together with some traces amounts of t,c-ZrO_2.

Subsequent formation of ZrC at 1673 K in respect to formation of SiC at 1573 K, is in accordance with thermodynamic predictions based on free-energy calculations [2,24,27,30], i.e. formation of SiC is favored at lower temperatures than that of ZrC.

At 1773 K (Fig. 10d), m-ZrO_2 phase is completely transformed into the ZrC. However, traces of t,c-ZrO_2 are still present. At 1873 K (Fig. 10e), only ZrC and SiC phases are present, reflections of t,c-ZrO_2 disappeared. Complete carbothermal reduction of $ZrSiO_4$ into the ZrC and SiC, as observed in Fig. 10d and e, can be approximately represented by the following reaction:

$$ZrSiO_{4(s)} + 7C_{(s)} = ZrC_{(s)} + SiC_{(s)} + 4CO_{(g)} + C_{(s)} \quad (19)$$

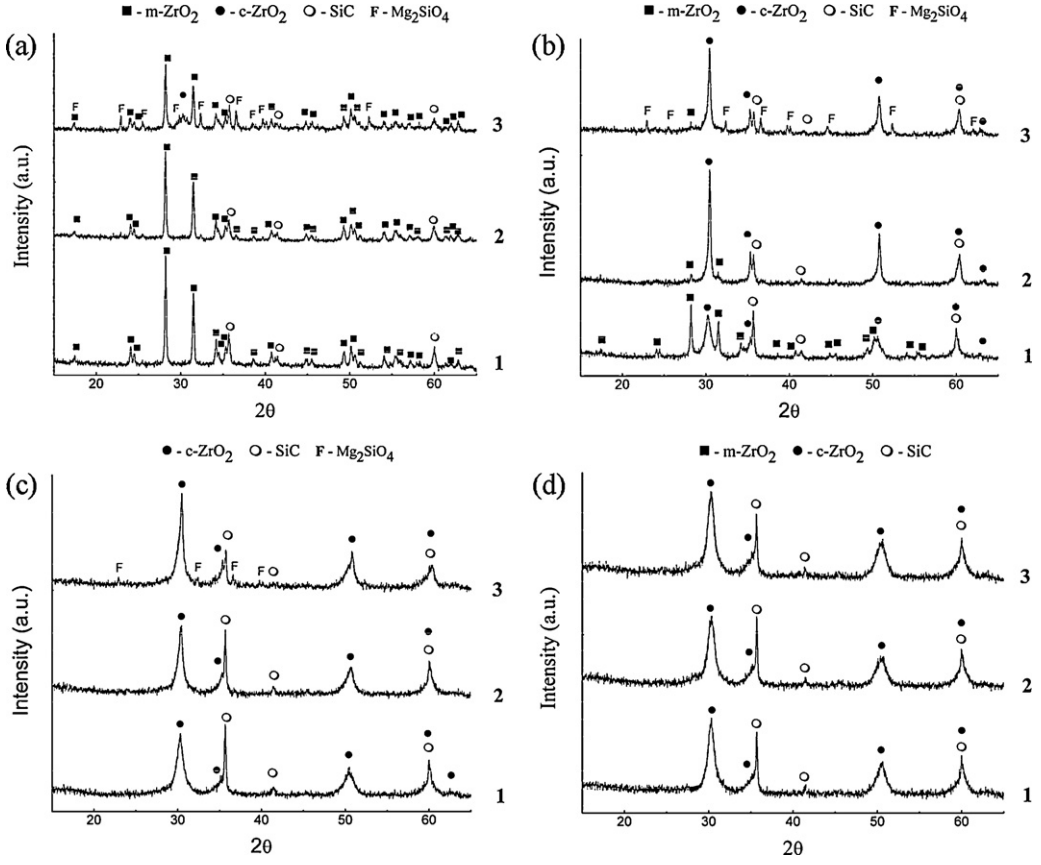

Fig. 14. XRD patterns of samples after decarburization at 873 K in air: (a) 1573 K, (b) 1673 K, (c) 1773 K, (d) 1873 K. (1 – 0% MgO; 2 – 10% MgO; 3 – 30% MgO).

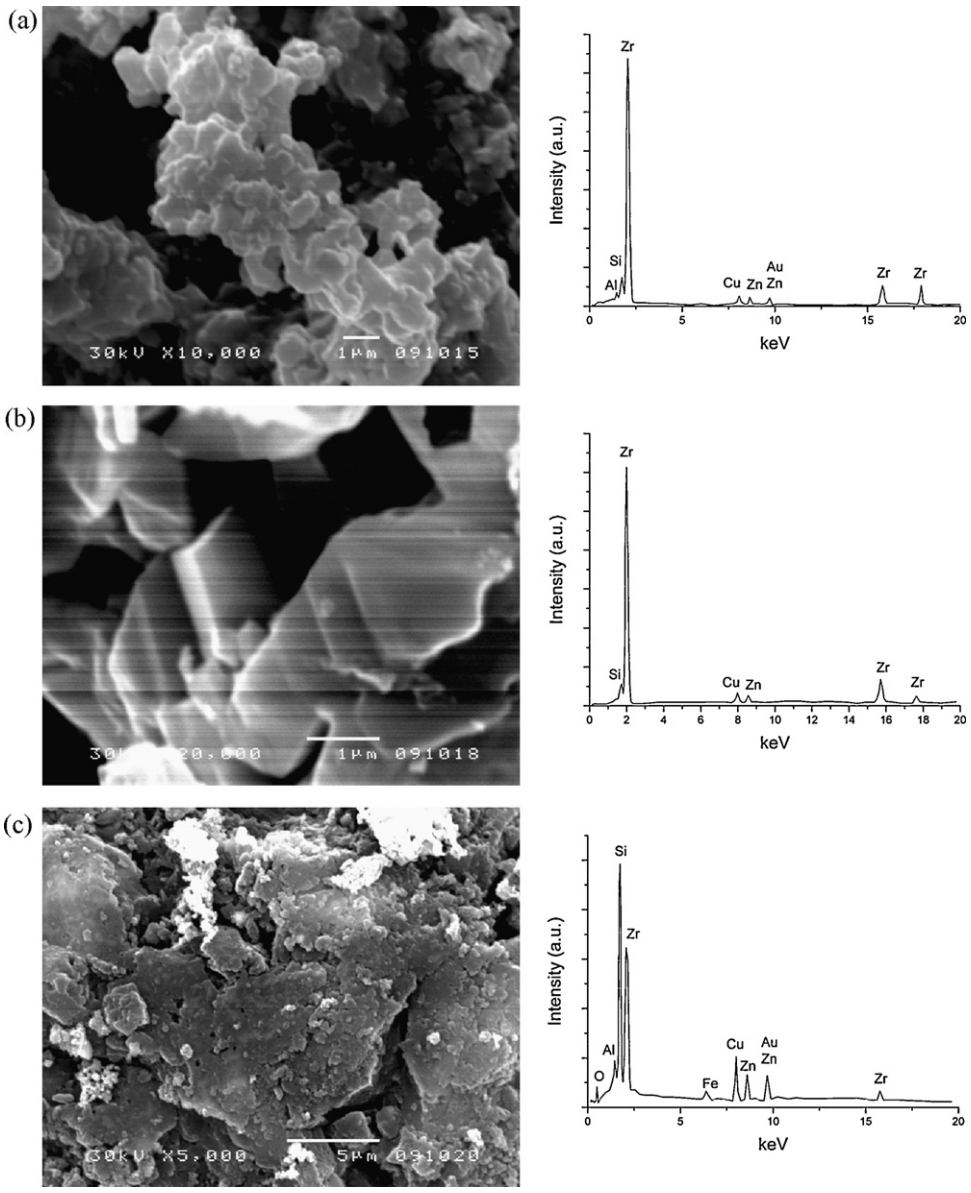

Fig. 15. SEM micrografs of samples heat treated at 1873 K, before decarburization, and their EDX spectra: (a) 0% MgO; (b) and (c) 30% MgO.

The percentage of weight loss expected by the reaction (19) is 41.9%, while experimentally observed weight losses are 43.2% (1773 K) and 46.7% (1873 K). After introducing the correction for activated carbon weight loss, expected weight loss value is 46.9%, which is in perfect agreement with weight loss observed at 1873 K This result is suggesting that the reaction is not finished at 1573 K.

The XRD patterns of $ZrSiO_4$/MgO samples, after the carbothermal reduction, are presented in Figs. 11–13. XRD patterns of samples with 5% and 10% MgO are quite similar to those obtained for sample without MgO addition. However, there is a difference in patterns obtained at 1673 K. In sample with 10% of MgO. It is seen that m-ZrO_2 phase completely disappeared, whilst diffraction lines of t,c-ZrO_2 phases are even stronger than for ZrC and SiC phases. The absence of forsterite reflections and the presence of strong sharp reflections of t,c-ZrO_2 indicate that most of MgO is used for stabilization of ZrO_2. Reflections positioned at $2\theta = 30.46^\circ$, 35.32°, 50.74° and 60.32° are carefully attributed to (1 1 1), (2 0 0), (2 2 0) and (3 1 1) reflections of c-ZrO_2 (JCPDS No. 27-0997). Additionally, the absence of some of the t-ZrO_2 reflections (like strong (2 0 2) reflection that should appear at 49,78°), confirms that observed ZrO_2 phase is indeed c-ZrO_2.

XRD patterns of samples with 30% MgO show quite different behaviour (Fig. 13). Reflections of ZrC and SiC are already observed at 1473 K, together with strong Mg_2SiO_4 and m-ZrO_2 reflections. Similar phase composition is observed at 1573 K with appearance of traces of c-ZrO_2 phase. At 1673 K, c-ZrO_2 and ZrC phases are dominant, SiC is obviously present while forsterite phase is diminishing. Observed 2θ values for c-ZrO_2 reflections are identical to those observed for c-ZrO_2 phase in sample with 10% MgO. With increasing temperature to 1773 K, ZrC phase becames dominant while forsterite phase completely disappeared. Reflections of c-ZrO_2 are still visible but their intensity is considerably reduced, confirming that at this temperature efficient carbothermal reduction of c-ZrO_2 is taking place. At 1873 K, ZrC and SiC phases are present, with only traces of c-ZrO_2.

The fact that formation of ZrC and SiC in this sample had already started at 1473 K, could be attributed to the cooperative catalytic effects of MgO and carbon on the decomposition of $ZrSiO_4$. In this

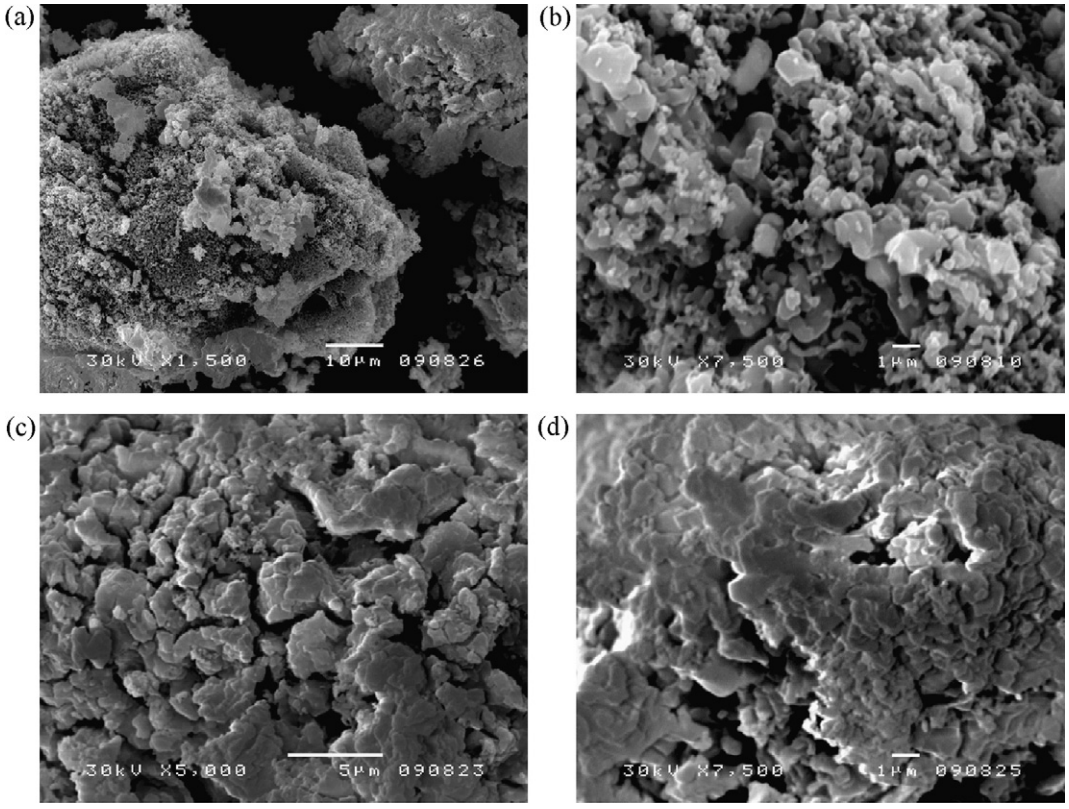

Fig. 16. SEM micrographs of sample with 0% MgO, heat treated at 1873 K, after decarburization in air (873 K, 2 h).

sample ZrO_2 is formed in greater amounts than in the sample without MgO and samples with 5% and 10% MgO added (Figs. 10a, 11a and 12a) due to the reaction (17), and thus carbothermal reduction of ZrO_2 can be observed earlier. Catalytic effect of high content of carbon has already been mentioned above (Fig. 10b and Fig. 1f). It also seems that it is easier to obtain SiC from Mg_2SiO_4 than from $ZrSiO_4$ (Fig. 10a–b and Fig. 13a), probably because of impurities present in our system (Al_2O_3, TiO_2, Fe_2O_3), in which low temperature eutectics [32] with Mg_2SiO_4 can be formed.

Disappearance of Mg_2SiO_4 at 1773 K can be explained, as proposed by Sugahara et al. [33], by reduction of forsterite in the presence of excess carbon, directly into the $SiO_{(g)}$ and $Mg_{(g)}$, which are then swept away by Ar flow:

$$Mg_2SiO_4 + 3C = SiO_{(g)} + 2Mg_{(g)} + 3CO_{(g)} \quad (20)$$

However, this reaction is also only an assumption, based on fact that no other Mg-containing phases are detected after disappearance of forsterite phase. Similar phenomena were observed during CTR processes of sepiolite and asbestos (natural Mg-silicates) [34–36].

From XRD patterns presented in Figs. 11–13, it can also be observed that c-ZrO_2 content increases with increasing MgO content. It seams that most of MgO added is incorporated into ZrO_2 lattice. That is why stabilized c-ZrO_2 is produced which is the dominant phase at 1673 K in samples with 10% and 30% MgO, contrary to sample without MgO addition.

XRD patterns of samples with and without MgO addition, after decarburization processes, are presented in Fig. 14. As had been seen before, due to oxidation at 873 K ZrC is transformed into the c-ZrO_2 in all samples. The m-ZrO_2 phase is present only in samples in which m-ZrO_2 was present before decarburization process. All samples heat treated at 1873 K (Fig. 14d) and samples with 0% and 10% MgO heat treated at 1773 K (Fig. 14c), contain only c-ZrO_2 and SiC phases.

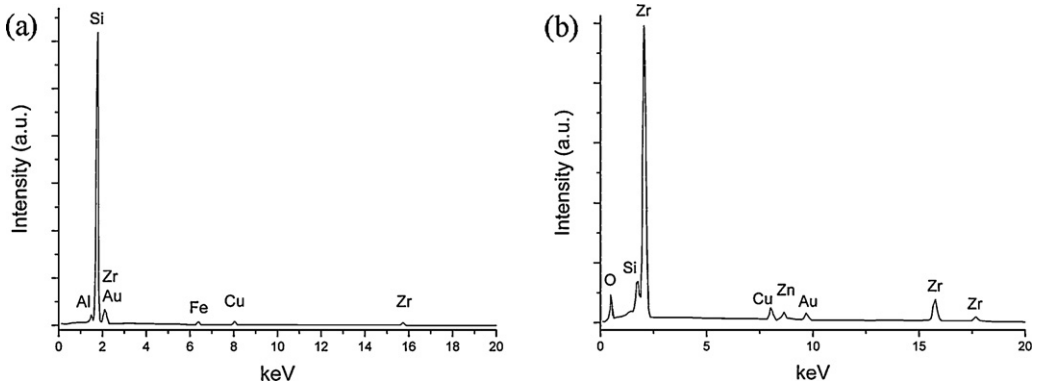

Fig. 17. EDX spectra of areas presented in: (a) Fig. 16b; (b) Fig. 16c and d.

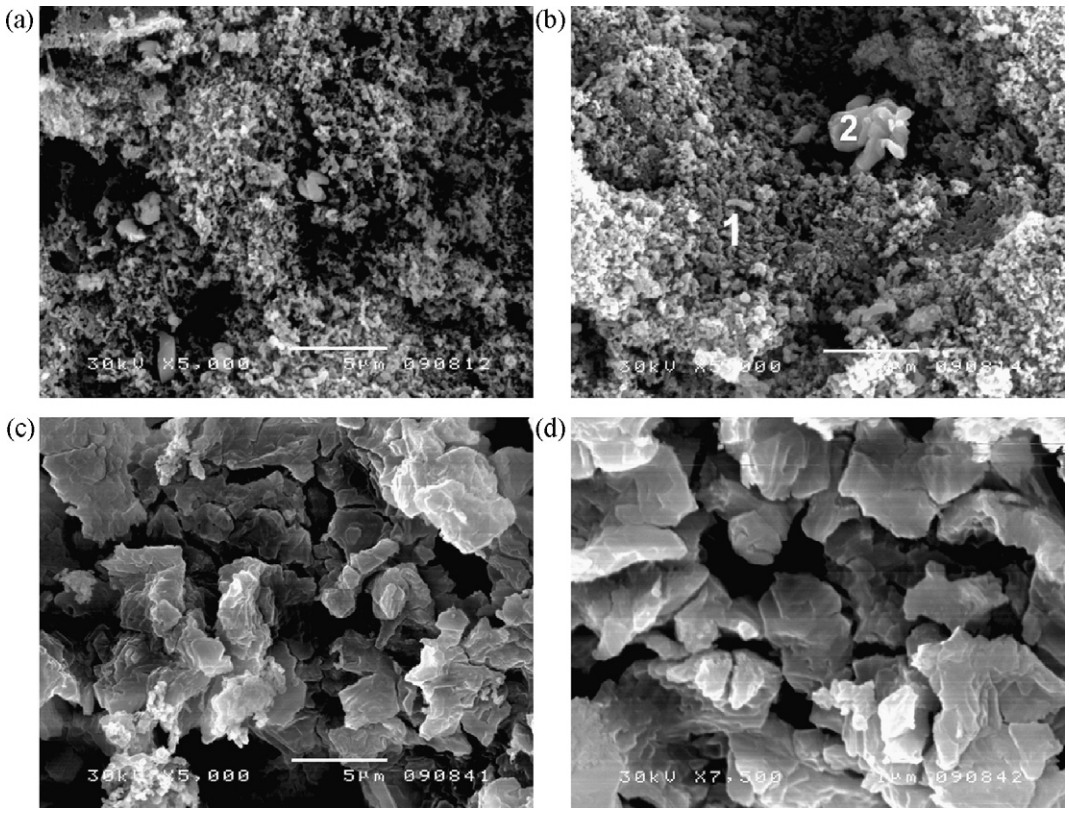

Fig. 18. SEM micrographs of sample with 30% MgO, heat treated at 1873 K, after decarburization in air (873 K, 2 h).

It is noteworthy to point out the fact that reflections of c-ZrO_2 in samples with MgO addition before decarburization processes are very sharp (≈0.2°), in contrast to those of c-ZrO_2 in samples after decarburization processes, which is obtained by ZrC oxidation (for example, ≈0.9° for samples heat treated at 1873 K, Fig. 14d). In samples after decarburization in which c-ZrO_2 was obtained by ZrC oxidation of c-ZrO_2, the reflections are not so sharp (for example, ≈0.9° for samples heat treated at 1873 K, Fig. 14d). Sharp reflections of c-ZrO_2 observed, too in samples with 10% and 30% MgO at 1673 K after decarburization (Fig. 14b), which indicates that this phase predominantly consisted of MgO stabilized c-ZrO_2 with only small contribution of c-ZrO_2 phase obtained by ZrC oxidation. This is consistent with phase composition of these samples before decarburization (Figs. 12c and 13c). In that case MgO stabilized c-ZrO_2 phase was also dominant over ZrC phase. At 1773 K (Figs. 12d and 13d) ZrC phase is dominant, and c-ZrO_2 reflections in decarburized samples became much wider (≈0.5–0.6°, Fig. 14c) indicating that this phase predominantly consisted of c-ZrO_2 obtained by ZrC oxidation. Finally, samples in which c-ZrO_2 is absent before decarburization process (1873 K, Figs. 12e and 13e) produce c-ZrO_2 phase which is completely obtained by ZrC oxidation and XRD patterns of these samples (Fig. 14d.2 and d.3) are identical to pattern of sample without MgO addition (Fig. 14d.1).

In conclusion, samples with MgO addition shows that some kind of catalytic effect really exists, but it is non-effective when regarding final temperature needed to obtain the desired products. MgO does stabilize the c-ZrO_2 phase during the $ZrSiO_4$ CTR process, but in order to obtain c-ZrO_2/SiC powder without Mg, same temperature is needed as in the sample without MgO addition. Obviously, it is then much simpler to just use excess carbon and completely transform $ZrSiO_4$ into the ZrC/SiC, and then by simple oxidation, to transform ZrC into the c-ZrO_2.

SEM micrographs and EDX spectra of samples with 0% and 30% MgO added and subjected to carbothermal reduction at 1873 K are presented in Fig. 15. Before decarburization, excess of free carbon makes visual examination and photographying of samples rather difficult. For that reason we present few pictures with characteristic phases which are illustrated in (Fig. 15a–c).

Fig. 15a and b, represents ZrC rich areas containing small amounts of SiC for samples prepared both with 0% and 30% of MgO. Total absence of O confirmes that these micrographs and their EDX spectra represent mixed carbide phase. Another mixed carbide phase, but this time rich in SiC, is presented in Fig. 15c: EDX spectra shows the presence of ZrC and SiC together with some impurities (Al, Fe) originating from as-received commercial $ZrSiO_4$ powder. Absence of Mg in EDX spectra of sample prepared with 30% MgO, confirms complete reduction of forsterite into the $Mg_{(g)}$ as previously observed by XRD analysis. Cu and Zn peaks are from brass sample carrier and Au peaks are due to Au coating of samples.

SEM micrographs and EDX spectra of samples with 0% and 30% MgO, after had been subjected to carbothermal reduction at 1873 K and then decarburization process, are presented in Figs. 16–19.

SEM micrographs of sample with 0% MgO, heat treated at 1873 K and then decarburized in air (873 K, 2 h) are presented in Fig. 16. Two different phases can be observed in this sample: phase consisting of loosen smaller particles (Fig. 16b) and phase consisting of bigger particles sintered together (Fig. 16c and d).

EDX spectra of phase presented in Fig. 16b is given in Fig. 17a: it represents SiC phase with small amount of ZrO_2 present, and traces of Al_2O_3. EDX spectra of phase presented in Fig. 16c and d is given in Fig. 17b: it represents ZrO_2 phase with small amount of SiC present.

SEM micrographs of sample with 30% MgO, heat treated at 1873 K and then decarburized in air (873 K, 2 h) are presented in Fig. 18. Two different phases, similar to those observed in sample with 0% MgO, can be observed in this sample too: phase consisting of loosen smaller particles (Fig. 18a and b, area noted as »1«) and phase consisting of bigger particles sintered together (Fig. 18b–d, area noted as »2«).

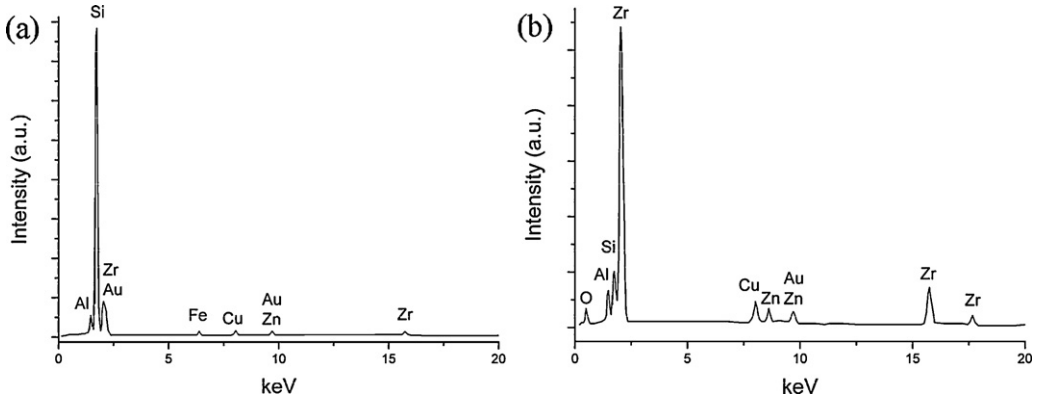

Fig. 19. EDX spectra of areas presented in: (a) Fig. 9a and b (area »1«); (b) Fig. 9c and d (area »2«).

EDX spectra representing phases presented in Fig. 18a and b (area noted as »1«), is given in Fig. 19a: it represents SiC phase with small amount of ZrO_2 present, and traces of Al_2O_3. EDX spectra of phase presented in Fig 18b–d (area noted as »2«), is given in Fig. 19b: it represents ZrO_2 phase with small amount of SiC present and traces of Al_2O_3.

As one can see, phases observed in samples prepared with both 0% and 30% MgO, are quite similar by morphology as well as by composition deduced from EDX spectra of these phases. This is quite in accordance with earlier observations made from XRD analysis. XRD patterns show no difference between these two samples.

The characteristic ZrO_2 polyhedron forms are distinguished in Fig. 16c and d and Fig. 18c and d. The average crystal size is $\geq$1 (m. Crystals tend to form clusters and it seems that many crystals of ZrO_2 are sintered together. They make aggregates which in self structure consist of more than 20 crystals. Although consisted of rather small crystallites ($\langle D \rangle \approx 10$ nm), c-ZrO_2 particles are much bigger ($\geq$1 μm) then we expected on the basis of crystallite size observed by XRD analysis.

Looser more porous phase, consisting of smaller particles irregular both in shape and size, is SiC phase. Appearance is very similar to SiC phases observed in samples obtained by CTR reaction of natural Mg-silicates (sepiolite, asbestos, [34–36]).

According to EDX spectra of these two phases, c-ZrO_2 and SiC phase are obviously quite well separated and consisted of large aggregates of particles.

4. Conclusions

It has been shown that it is possible to obtain pure (or almost pure) m-ZrO_2 and c-ZrO_2 powders, as well as c-ZrO_2/SiC mixed composite powders after the heat treatment of zircon at relatively low temperatures. Process is relatively simple, consisting of two steps (carbothermal reduction/decarburization). It was shown that by altering the C/$ZrSiO_4$ ratio, various products can be obtained. For low carbon content (1:1) m-ZrO_2 is obtained, for larger carbon content (5:1) almost pure c-ZrO_2 is obtained, and for excess carbon content (7:1) c-ZrO_2/SiC mixed powders are obtained. Mixed composite powders, especially of this composition, have a potential for making good structural ceramics with improved mechanical properties.

Samples with MgO addition show that some kind of catalytic effect does exists, but it is non-effective when final temperature needed to obtain the desired products is taken into account.

Acknowledgment

This project was financially supported by the Ministry of Science and Environmental Protection of Serbia (project number: 45012).

References

[1] K. Komeya, in: S. Saito (Ed.), Fine Ceramics, Elsevier Sci. Publ. Co, New York, 1988, p.175.
[2] S. De Souza, B.S. Terry, J. Mater. Sci. 29 (1994) 3329–3336.
[3] F.K. Van Dijen, R. Metselaar, J. Eur. Ceram. Soc. 7 (1991) 177–184.
[4] A.C.D. Chaklader, S. Das Gupta, E.C.Y. Lin, J. Am. Ceram. Soc. 75 (1992) 2283–2285.
[5] A.D. Mazzoni, E.F. Aglietti, Mater. Chem. Phys. 37 (1994) 344–348.
[6] D.H. Filsinger, D.B. Bourrie, J. Am. Ceram. Soc. 73 (1990) 1726–1732.
[7] L. Combemale, Y. Leconte, X. Portier, N. Herlin-Boime, C. Reynaud, J. Alloys Compd. 483 (2009) 468–472.
[8] K. Das, T.K. Bandyopadhyay, Mater. Sci. Eng. A 379 (2004) 83–91.
[9] B.P. Das, M. Panneerselvam, K.J. Rao, J. Solid State Chem. 173 (2003) 196–202.
[10] T. Ishigaki, S.M. Oh, J.G. Li, D.W. Park, Sci. Technol. Adv. Mater. 6 (2005) 111–118.
[11] H. Li, L. Zhang, L. Cheng, Y. Wang, Ceram. Int. 35 (2009) 2831–2836.
[12] J.C. Kim, B.K. Kim, Scripta Mater. 50 (2004) 969–972.
[13] D.W. Lee, J.H. Yu, B.K. Kim, T.S. Jang, J. Alloys Compd. 449 (2008) 60–64.
[14] B. Debalina, M. Kamaraj, B.S. Murthy, S.R. Chakravarthi, R. Sarathi, J. Alloys Compd. 496 (2010) 122–128.
[15] A. Kaiser, M. Lobert, R. Telle, J. Eur. Ceram. Soc. 28 (2008) 2199–2211.
[16] S. Shimada, Solid State Ionics 101–103 (1997) 749–753.
[17] T.Y. Luo, T.X. Liang, C.S. Li, Mater. Sci. Eng. A 366 (2004) 206–209.
[18] S. Kikkawa, A. Kijima, K. Hirota, O. Yamaguchi, Solid State Ionics 151 (2002) 359–364.
[19] S. Kikkawa, A. Kijima, K. Hirota, O. Yamamoto, J. Am. Ceram. Soc. 85 (2002) 721–723.
[20] X.-J. Jin, Curr. Opin. Solid State Mater. Sci. 9 (2005) 313–318.
[21] J. Widoniak, S. Eiden-Assmann, G. Maret, Eur. J. Inorg. Chem. (2005) 3149–3155.
[22] E. Djurado, P. Bouvier, G. Lucazeau, J. Solid State Chem. 149 (2000) 399–407.
[23] P.K. Panda, L. Mariappan, V.a. Jaleel, T.S. Kannan, A. Amroune, J. Dubois, G. Fantozzi, J. Mater. Sci. 31 (1996) 4277–4288.
[24] B.-Y. Ma, J.-K. Yu, Trans. Nonferrous Met. Soc. China 17 (2007) 996–1000.
[25] N. Rigopoulos, A. Oh, M. Yousuff, R.G. O'Donnell, M.B. Trigg, J. Aust. Ceram. Soc. 45 (2009) 54–58.
[26] B.-Y. Ma, J. Yu, J. Rare Earths 27 (2009) 806–810.
[27] B.-Y. Ma, J.-K. Yu, Q. Zhu, Y. Sun, Int. J. Miner. Metall. Mater. 16 (2009) 581–585.
[28] G.C. Wei, J. Am. Ceram. Soc. 66 (1983) C-111–C-113.
[29] V.D. Krstić, J. Am. Ceram. Soc. 75 (1992) 170–174.
[30] A. Maitre, P. Lefort, Solid State Ionics 104 (1997) 109–122.
[31] P. Scherrer, Göttinger Nachrichten Gesell. 2 (1918) 98–100.
[32] N.A. Toropov, V.P. Barzakovskij, V.V. Lapin, N.N. Kurceva, Diagrammy sostoyaniya silikatnyh sistem, Nauka, Lenjingrad, 1969.
[33] Y. Sugahara, K. Kuroda, C. Kato, J. Mater. Sci. Lett. 4 (1985) 928–931.
[34] A. Devečerski, A. Radosavljević-Mihajlović, A. Egelja, M. Pošarac, B. Matović, Mater. Sci. Forum 555 (2007) 261–265.
[35] A. Devečerski, M. Pošarac, A. Egelja, I. Pongrac, A. Radosavljević-Mihajlović, B. Matović, J. Optoelectron. Adv. Mater. 10 (2008) 876–879.
[36] A. Devečerski, M. Pošarac, A. Egelja, A. Radosavljević-Mihajlović, S. Bošković, M. Logar, B. Matović, J. Alloys Compd. 464 (2008) 270–276.